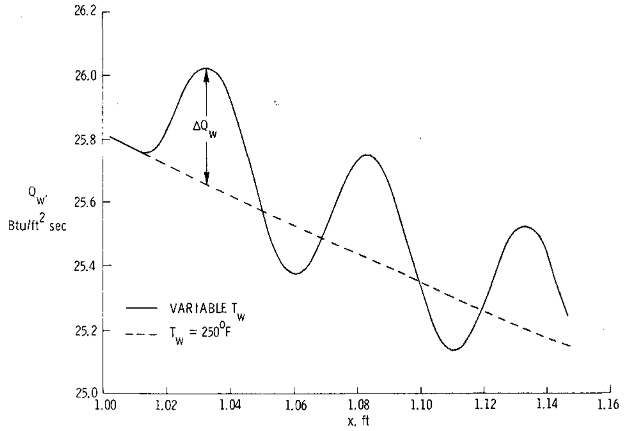

Fig. 2 Heat transfer results for typical case $R(x_w) = 1.34 \times 10^6$ ft^{-1}, $\Delta T_w = 25°$F, $w = 0.05$ ft, $x_w = 1.00$ ft.

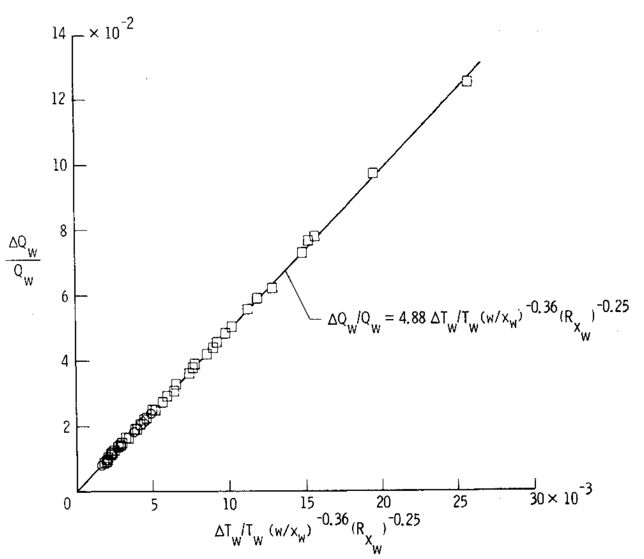

Fig. 3 Correlation of cyclic wall temperature results.

of Ref. 2 as to the magnitude of ΔQ_w. These results, of course, lack experimental verification.

An attempt was made to correlate the results of the cyclic wall temperature cases in terms of the maximum deviation of heating rate, ΔQ_w, from the constant wall temperature data such as $\Delta T_w/T_w$, w, x_w, R_w, and $R(x_w)$. In order to assist in correlating these data, several cases were run in which the values of $\Delta T_w/T_w$ and w are outside the range of practicality for actively cooled transports. In all a total of 50 cases were analyzed. The result for one apparently successful correlation is shown in Fig. 3. The straight line faired through the 50 data points has the equation

$$\frac{\Delta Q_w}{Q_w} = 4.88\,\frac{\Delta T_w}{T_w}\left(\frac{w}{x_w}\right)^{-0.36}\left(R_{x_w}\right)^{-0.25}$$

Using this correlation one sees that it is possible to have rather large variations in the heat transfer rate due to a cyclic wall temperature distribution. However, when one examines the result for values of $(\Delta T_w/T_w)$, w, x_w, and $R(x_w)$ that are practical for a Mach 8 aircraft, the variation in heat transfer rate is less than about six percent which is believed sufficiently small so that there is no need to couple the conductive thermal analysis used for panel design with a boundary-layer program.

References

[1]Becker, J. V., "Prospects for Actively Cooled Hypersonic Transports," *Aeronautics and Astronautics*, Vol. 9, No. 8, Aug. 1971, pp. 32–39.

[2]Helenbrook, R. G. and Anthony, F. M., "Design of a Convective Cooling System for a Mach 6 Hypersonic Transport Airframe," CR-1918, Dec. 1971, NASA.

[3]Anderson, E. C. and Lewis, C. H., "Laminar or Turbulent Boundary Layer Flows of Perfect Gases or Reacting Gas Mixtures in Chemical Equilibrium," CR-1893, Oct. 1971, NASA.

[4]Price, J. M. and Harris, J. E., "Computer Program for Solving Compressible Nonsimilar-Boundary-Layer Equations for Laminar, Transitional, or Turbulent Flows of a Perfect Gas," TM X-2458, April 1972, NASA

Calculation of Nonlinear Lift and Pitching Moment Coefficients for Slender Wing-Body Combinations

H. Otto*

Deutsche Forschungs- und Versuchsanstalt für Luft- und Raumfahrt (DFVLR), Forschungszentrum Braunschweig, F. R. Germany

Nomenclature

U_∞ = freestream velocity
α = angle of incidence
b = wing span
$\bar{c}$ = mean wing chord = S/b
$\bar{\bar{c}}$ = mean aerodynamic chord = $\frac{1}{S}\int_{-b/2}^{+b/2} c^2(y)dy$
S = wing area
A = aspect ratio
λ = taper ratio
ν = kinematic viscosity
Re = Reynolds number = $U_\infty \bar{c}/\nu$
C_L = lift coefficient = $L/(\rho(U_\infty^2)S/2)]$
C_m = pitching moment coefficient = $M/(\rho(U_\infty^2)S\bar{\bar{c}}/2)$, nose-up positive, referred to the quarter-chord point of the mean aerodynamic chord projected on the plane of symmetry, N_{25}

Introduction

IT is well known that lift and pitching moment coefficients of slender wings and fuselages depend nonlinearly on the angle of incidence.[1,2] This behavior is related to flow separation which leads to the formation of trailing vortices above the upper surface of such wings and bodies. The nonlinearities arise from the fact that the position of the trailing vortices with respect to the wing and the body changes with the angle of incidence.

For combinations of slender wings and fuselages very strong interference effects have to be expected and the occurrence of nonlinear lift and pitching moment coefficients may result from the following effects: 1) effect of the wing vortices on the wing, 2) interference effect of the wing vortices on the fuselage, 3) effect of the fuselage vortices on the fuselage, and 4) interference effect of the fuselage vortices on the wing. The effect 1) has been dealt

Received March 14, 1974.
Index categories: Subsonic and Transonic Flow; LV/M Aerodynamics.

*Research Scientist, Low Speed Wind Tunnel Division.

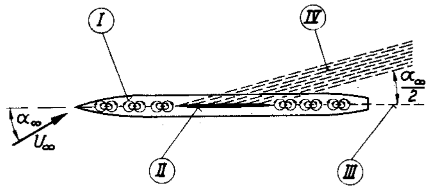

Fig. 1 Wing-body combination: Distribution of singularities after linear and nonlinear theory. (I) Doublet distribution along the fuselage centerline. (II) Vortex distribution in the wing plane. (III) Trailing vortices in the wing plane = linear theory.[3] (IV) Trailing vortices inclined against the wing plane = present nonlinear theory.[4]

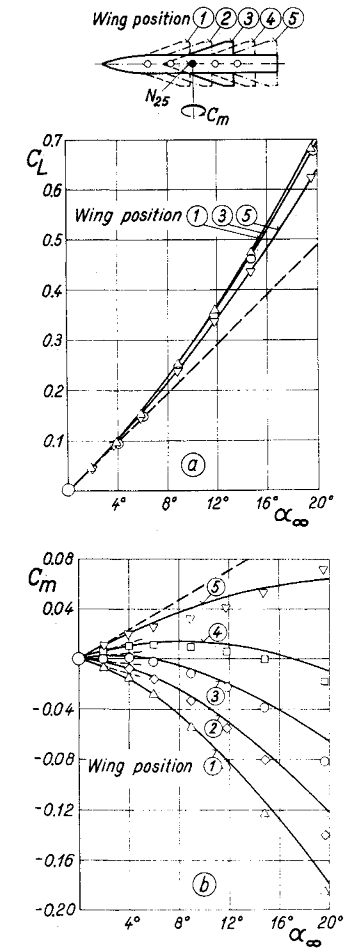

———— present nonlinear theory[4]

- - - - - - linear theory, Hafer[3]

experiment	wing position
△	①
◇	②
○	③
□	④
▽	⑤

Fig. 2 Aerodynamic coefficients for a slender body mid-wing configuration at different rear positions of the wing, $Re = 1.9 \times 10^6$. a) Lift curves, $C_L(\alpha_\infty)$. b) Pitching moment curves, $C_m(\alpha_\infty)$.

with by Gersten[1,2] for small aspect ratio wings. The interference effect 2) has been treated by Hafer[3] for wings of large aspect ratio. Here we propose to deal with both effects for wings of small aspect ratio.[4]

Experimental Investigations

These influences have been studied by means of an extensive experimental research program. Three component wind-tunnel measurements as well as flow investigations have been carried out on various slender wings, fuselages, and their combinations. Three sharp-edged wings of aspect ratio $A = 1$ and of taper ratios $\lambda = 1$ (rectangular wing), $\lambda = 0.5$ (trapezoidal wing), and $\lambda = 0.125$ (cropped delta wing) have been investigated. The five fuselages used in the tests had thickness/length ratios of 0.05 and 0.10, and were cylindrical bodies with various shapes of the nose and of the afterbody. The wing-body combinations had body-thickness wing-span ratios of 0.2 and 0.4. The wings were located at the centerline of the fuselages and their rear position was altered in a wide range.

The experimental investigations have shown that the effects of the fuselage vortices, effects 3 and 4, are small compared with those of the wing vortices, effects 1 and 2. In addition to the well-known effect of the wing vortices on the wing itself, effect 1, for wing-body combinations an interference effect turned out to be important which mainly results from the influence of the wing vortices on that part of the fuselage which is located behind the wing, effect 4. Therefore, if the rear position of the wing with respect to the fuselage is increased, this interference effect decreases and the nonlinear portions of the lift coefficients and especially of the pitching moment coefficients are reduced.

Theoretical Investigations

Considering these experimental results, the linear theory of lifting wing-body combinations after Hafer[3] has been extended to the calculation of nonlinear lift and pitching moment coefficients of slender wing-body combinations. In this approach, the fairly weak trailing vortices of the fuselage were neglected and only the influences of the trailing vortices of the wing have been taken into account. In the linear theory of Hafer, the fuselage is represented by a distribution of doublets along the center line of the fuselage. The wing is replaced by a continuous vortex distribution and a trailing vortex sheet which are located in the plane of the wing as indicated in Fig. 1 by configurations I–III. This leads to a linear dependence of the aerodynamic coefficients on the angle of incidence. In the present nonlinear lifting wing-body theory,[4] the wing is represented by the vortex model of the nonlinear lifting-surface theory after Gersten as given by configuration IV in Fig. 1. In this theory the trailing vortices are located in sheets inclined at an angle of $\alpha_\infty/2$ with respect to the wing plane. For this vortex model the effect of the trailing vortices on the wing can be calculated by means of the nonlinear theory after Gersten.[1,2] In order to determine the interference effect of the trailing vortices on the fuselage, a new method for calculating the induced velocities at the fuselage centerline has been developed. The present calculation procedure is similar to that applied by Hafer; i.e., the induced velocities produced by the wing at the fuselage centerline and by the fuselage at the wing surface are taken into account simultaneously.

In Fig. 2, some results of calculations after the present nonlinear theory for a slender body mid-wing configuration at different rear positions of the wing with respect to the fuselage are compared with experimental results. The configuration consists of a cylindrical body with an ogival nose and the cropped delta wing of aspect ratio $A = 1$ and taper ratio $\lambda = 0.125$. Furthermore, the results of the linear theory after Hafer are shown for comparison.

In Fig. 2a the lift curves $C_L(\alpha_\infty)$ are plotted for the most forward wing position ①, the medium wing position ③, and the most rearward wing position ⑤. Comparison between theory and experiment shows that the experimental data are well predicted by the present nonlinear theory for all rear positions of the wing, whereas the results of the linear theory show good agreement for very small angles of incidence only. The pitching moment curves $C_m(\alpha_\infty)$ are plotted in Fig. 2b for five different rear positions of the wing. The present nonlinear theory gives excellent agreement with the experimental data for all wing positions. The improvement achieved by the nonlinear theory compared with the linear theory is remarkable.

The results of sample calculations carried out on slender body mid-wing configurations for other body shapes and other wing plan forms show also fairly good agreement with experimental results.[4]

References

[1]Gersten, K., "Nichtlineare Tragflächentheorie, insbesondere für Tragflügel mit kleinem Seitenverhältnis," Habilitationsschrift Braunschweig 1960. *Ingenieur Archiv*, Vol. 30, 1961, pp. 431–452.

[2]Gersten, K., "A Nonlinear Lifting-Surface Theory Especially for Low-Aspect-Ratio Wings," *AIAA Journal*, Vol. 1, No. 4, April 1963, pp. 924–925.

[3]Hafer, X., "Untersuchungen zur Aerodynamik der Flügel-Rumpf-Anordnungen," Dissertation Braunschweig, 1957. Jahrbuch 1957 der Wissenschaftlichen Gesellschaft für Luftfahrt (WGL), 1958, pp. 191–207.

[4]Otto, H., "Ein Beitrag zu den nichtlinearen Auftriebs- und Nickmomenteneigenschaften von schlanken Flügel-Rumpf-Kombinationen," Dissertation Braunschweig, 1972. Bericht 72/7 des Institutes für Strömungsmechanik der Technischen Universität Braunschweig, 1972; also Deutsche Luft- und Raumfahrt (DLR), Forschungsbericht (FB) 73-66, 1973; and Zeitschrift für Flugwissenschaften (ZFW), Vol. 22, 1974, pp. 187–200.

Some Characteristics of Airfoil-Jet Interaction with Mach Number Nonuniformity

C. Edward Lan*

The University of Kansas, Lawrence, Kan.

Introduction

A STOL concept of current interest is the upper surface blowing configuration where the high-velocity jet from high-bypass-ratio engines blows over the wing surface. The high lift derives not only from the Coanda effect when the flap is deflected, but also from the aerodynamic interaction with the relatively thick jet. Shollenberger[1] has analyzed a similar configuration including the effects of 2-D nacelle and jet distortion. The case where the airfoil is in a midstream of one velocity with different velocity regions above and below has been treated by Ting and Liu.[2] In both investigations the flow has been assumed 2-D, inviscid, and incompressible. The effect of Mach number nonuniformity where the jet Mach number is different from the freestream value has not been investigated. The Mach number nonuniformity may occur not only at low speed with high thrust but also at high-speed cruise flight.

Received April 11, 1974; revision received May 6, 1974. This research is part of a project supported by NASA Grant 17-002-107.

Index category: Aircraft Aerodynamics (Including Component Aerodynamics).

*Associate Professor of Aerospace Engineering. Member AIAA.

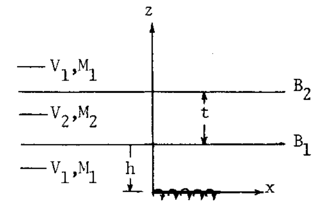

Fig. 1 Geometry definition.

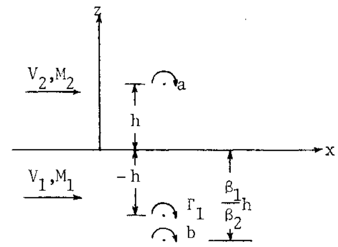

Fig. 2 Vortex images.

In this Note, the image method will be used to examine the upper-surface-blowing jet-airfoil interaction with Mach number nonuniformity. The formulation represents an extension of the classical incompressible results.[2,3] Some characteristics of the interaction will be discussed. The main assumptions are 1) inviscid linear theory, 2) two-dimensional jet, 3) no turbulent mixing, and 4) no airfoil thickness effect.

Mathematical Formulation

A plane jet with Mach number M_2 is assumed to be imbedded in a freestream of Mach number M_1. A thin airfoil is placed at a distance h below the lower jet surface, as shown in Fig. 1. For $h = 0$, this may represent an idealized configuration with upper-surface blowing jet. The induced velocity vector due to a two-dimensional vortex with strength Γ in the linearized compressible flow can be shown to be[4]

$$\mathbf{q} = (\Gamma\beta/2\pi)(\mathbf{i}(z - z') - \mathbf{k}(x - x'))/((x - x')^2 + \beta^2(z - z')^2) \quad (1)$$

where $\beta = (1 - M^2)^{1/2}$. To examine how disturbances reflect and diffract at the interface of two flows of different energy levels, consider a vortex of Γ_1 at $z' = -h$ in region 1 (See Fig. 2). The boundary conditions at $z = 0$ are[3]

$$w_1/V_1 = w_2/V_2 \quad \text{(Flow tangency)} \quad (2)$$

$$\rho_1 V_1 u_1 = \rho_2 V_2 u_2 \quad \text{(Pressure continuity)} \quad (3)$$

Because of the presence of the vortex Γ_1 at $(x', -h)$, the flowfield in region 2 will be disturbed. Following Koning's concept[3] for incompressible flow, a vortex of strength b at $z' = -\beta_1 h/\beta_2$ will be introduced. It follows that the induced flow in region 2 can be written as

$$\mathbf{q}_2 = \frac{b\beta_2}{2\pi}\frac{\mathbf{i}(z + \beta_1 h/\beta_2) - \mathbf{k}(x - x')}{(x - x')^2 + \beta_2^2(z + \beta_1 h/\beta_2)^2} \quad (4)$$

On the other hand, the disturbance due to the vortex Γ_1 will be reflected back to region 1 at the interface, as represented by a vortex of strength "a" at the image point in region 2. Hence, the total induced flow in region 1 is

$$\mathbf{q}_1 = \frac{\Gamma_1\beta_1}{2\pi}\frac{\mathbf{i}(z + h) - \mathbf{k}(x - x')}{(x - x')^2 + \beta_1^2(z + h)^2} + \frac{a\beta_1}{2\pi}\frac{\mathbf{i}(z - h) - \mathbf{k}(x - x')}{(x - x')^2 + \beta_1^2(z - h)^2} \quad (5)$$

Using Eqs. (4) and (5) together with Eqs. (2) and (3), the unknown vortex strengths a and b can be found to be